ARTICLE

CC2D2A Is Mutated in Joubert Syndrome and Interacts with the Ciliopathy-Associated Basal Body Protein CEP290

Nicholas T. Gorden,[1,20] Heleen H. Arts,[8,20] Melissa A. Parisi,[1] Karlien L.M. Coene,[8] Stef J.F. Letteboer,[8] Sylvia E.C. van Beersum,[8] Dorus A. Mans,[8] Abigail Hikida,[1] Melissa Eckert,[9] Dana Knutzen,[1] Abdulrahman F. Alswaid,[10] Hamit Özyurek,[11] Sel Dibooglu,[12] Edgar A. Otto,[13] Yangfan Liu,[14] Erica E. Davis,[14] Carolyn M. Hutter,[2] Theo K. Bammler,[3] Frederico M. Farin,[3] Michael Dorschner,[4] Meral Topçu,[15] Elaine H. Zackai,[16] Phillip Rosenthal,[17] Kelly N. Owens,[5,6,7] Nicholas Katsanis,[14] John B. Vincent,[18] Friedhelm Hildebrandt,[13] Edwin W. Rubel,[5,6] David W. Raible,[6,7] Nine V.A.M. Knoers,[8] Phillip F. Chance,[1] Ronald Roepman,[8] Cecilia B. Moens,[19] Ian A. Glass,[1] and Dan Doherty[1,*]

Joubert syndrome and related disorders (JSRD) are primarily autosomal-recessive conditions characterized by hypotonia, ataxia, abnormal eye movements, and intellectual disability with a distinctive mid-hindbrain malformation. Variable features include retinal dystrophy, cystic kidney disease, and liver fibrosis. JSRD are included in the rapidly expanding group of disorders called ciliopathies, because all six gene products implicated in JSRD (*NPHP1*, *AHI1*, *CEP290*, *RPGRIP1L*, *TMEM67*, and *ARL13B*) function in the primary cilium/basal body organelle. By using homozygosity mapping in consanguineous families, we identify loss-of-function mutations in *CC2D2A* in JSRD patients with and without retinal, kidney, and liver disease. *CC2D2A* is expressed in all fetal and adult tissues tested. In ciliated cells, we observe localization of recombinant CC2D2A at the basal body and colocalization with CEP290, whose cognate gene is mutated in multiple hereditary ciliopathies. In addition, the proteins can physically interact in vitro, as shown by yeast two-hybrid and GST pull-down experiments. A nonsense mutation in the zebrafish *CC2D2A* ortholog (*sentinel*) results in pronephric cysts, a hallmark of ciliary dysfunction analogous to human cystic kidney disease. Knockdown of *cep290* function in *sentinel* fish results in a synergistic pronephric cyst phenotype, revealing a genetic interaction between *CC2D2A* and *CEP290* and implicating CC2D2A in cilium/basal body function. These observations extend the genetic spectrum of JSRD and provide a model system for studying extragenic modifiers in JSRD and other ciliopathies.

Introduction

Joubert syndrome and related disorders (JSRD [MIM 213300]) encompass a group of conditions characterized by hypotonia, ataxia, abnormal eye movements, and intellectual disability with a mid-hindbrain brain malformation giving the appearance of a molar tooth on brain imaging (the molar tooth sign [MTS]).[1] Other, more variable, clinical features include retinal dystrophy, coloboma, polydactyly, cystic renal disease, hepatic fibrosis, and other brain malformations that have been used to define clinical subtypes of JSRD such as COACH (cerebellar vermis hypoplasia, oligophrenia, ataxia, coloboma, and hepatic fibrosis [MIM 216360]).[2] Thus far, mutations in six genes (*NPHP1* [MIM 607100], *AHI1* [MIM 608894], *CEP290* [MIM 610142], *RPGRIP1L* [MIM 610937], *TMEM67* [MIM 609884], and *ARL13B* [MIM 608922]) have been identified in patients with JSRD and all of the gene products have been implicated in the function of the primary cilium/basal body.[1,3–13] JSRD are therefore included in the expanding group of disorders resulting from ciliary dysfunction, including Meckel syndrome (MKS [MIM 249000]), Bardet-Biedl syndrome (BBS [MIM 209900]), nephronophthisis (MIM 256100), and Leber congenital amaurosis (LCA [MIM 204000]). These disorders, termed ciliopathies,[14] share both phenotypic features (retinal dystrophy, polydactyly, cystic renal disease, and hepatic fibrosis) and molecular causes.[14,15] For example, mutations in the gene encoding the centrosomal and

[1]Division of Genetics and Developmental Medicine, Department of Pediatrics, School of Medicine, [2]Department of Epidemiology, School of Public Health, [3]Department of Environmental and Occupational Health Sciences, School of Public Health, [4]Division of Medical Oncology, Department of Medicine, School of Medicine, [5]Department of Otolaryngology-Head and Neck Surgery, School of Medicine, [6]Department of Biological Structure, [7]Virginia Merrill Bloedel Hearing Research Center, University of Washington, Seattle, WA 98195, USA; [8]Department of Human Genetics, Radboud University Nijmegen Medical Centre and Nijmegen Centre for Molecular Life Sciences, 6500 HB Nijmegen, The Netherlands; [9]Department of Evolution and Ecology, University of California, Davis, Davis, CA 95616, USA; [10]Department of Pediatrics, King Abdulaziz Medical City, Riyadh 111426, Saudi Arabia; [11]Department of Pediatrics, Ondokuz Mayis University, 55139 Kurupelit, Samsun, Turkey; [12]Department of Economics, 408 SSB, University of Missouri St. Louis, St. Louis, MO 63121, USA; [13]Department of Pediatrics, University of Michigan Health System, Ann Arbor, MI 48109-5640, USA; [14]McKusick-Nathans Institute of Genetic Medicine and Departments of Ophthalmology and Molecular Biology and Genetics, John Hopkins University, Baltimore, MD 21205, USA; [15]Department of Child Neurology, Hacettepe Children's Hospital, 06100 Ankara, Turkey; [16]Clinical Genetics Center, University of Pennsylvania School of Medicine, Genetics and Molecular Biology, The Children's Hospital of Philadelphia, Philadelphia, PA 19104, USA; [17]Departments of Pediatrics and Surgery, University of California, San Francisco, San Francisco, CA 94143-0136, USA; [18]Neurogenetics Section, Centre for Addiction and Mental Health, Toronto, ON M57 1R8, Canada; [19]Howard Hughes Medical Institute and Fred Hutchinson Cancer Research Center, Seattle, WA 98109, USA
[20]These authors contributed equally to this work
*Correspondence: ddoher@u.washington.edu
DOI 10.1016/j.ajhg.2008.10.002.

basal body protein CEP290 cause a spectrum of overlapping phenotypes including JSRD, MKS, LCA, and BBS, and loss of *CEP290* function causes cilium defects in mammalian cells.[5,16–20] The human phenotypes, including kidney cysts, are partially recapitulated in a zebrafish model for loss of *CEP290* function.[5]

In this work, we report mutations in the *CC2D2A* gene (MIM 612013) as a cause of JSRD in a substantial subset of a large, unselected JSRD cohort, including mutations associated with the distinctive COACH subtype. *CC2D2A* encodes a coiled-coil and C2 domain protein with predicted structural similarity to RPGRIP1 (MIM 605446) and RPGRIP1L, proteins known to be involved in LCA and JSRD/MKS, respectively;[3,4,21] however, little is known about the function of these proteins. Recently, *CC2D2A* mutations have been associated with autosomal-recessive mental retardation with retinitis pigmentosa (now known to be Joubert syndrome) and MKS.[22,23] In addition, we show that loss of *CC2D2A* function in the zebrafish mutant *sentinel* leads to the development of pronephric cysts, a hallmark of cilium dysfunction. Further, we show that CC2D2A colocalizes at the basal bodies of cilia and physically interacts with CEP290. This interaction is likely to be physiologically relevant, because suppression of *cep290* function in zebrafish significantly enhances the pronephric cyst phenotype of the *sentinel* mutant. This work extends the phenotypic spectrum caused by *CC2D2A* mutations to include JSRD and indicates that CC2D2A functions with CEP290 in the primary cilium/basal body protein network.

Material and Methods

Subjects

Subjects were recruited worldwide and collected under the approval of the Human Subjects Divisions at the University of Washington, the University of Michigan, and Johns Hopkins University. Characteristic brain-imaging findings, combined with developmental delay and ataxia, were the minimal criteria for JSRD, whereas subjects with BBS were ascertained as described by Beales et al.[24] Cerebellar vermis hypoplasia was a sufficient imaging criterion in subjects not evaluated by MRI. Known genes and loci for JSRD (*AHI1*, *CEP290*, *NPHP1*, *TMEM67*, chromosomal loci 9q34, and 11p11.2–q12.1) were excluded in the consanguineous families by either haplotype analysis for homozygosity via microsatellite markers or by direct sequencing. Nonconsanguineous families with mutations in *NPHP1* and *AHI1* were also excluded from the analysis.

SNP and Microsatellite Marker Genotyping

Single nucleotide polymorphisms (SNPs) were genotyped with the GeneChip Human Mapping 50K Array *Xba* 240 (Affymetrix Inc., Santa Clara, CA) under standard conditions. The arrays were scanned with a GeneChip Scanner 3000 and calls were assigned with GeneChip Operating Software (GCOS) and Genotyping Analysis Software. Overlapping homozygous intervals were identified with Excel (Microsoft Corporation, Redmond, WA) and shared haplotypes were identified with Stata Corp. (College Station, TX; code available on request). Microsatellite markers on chromosome 4p15 were genotyped with ABI primers and an ABI PRISM 3100 Genetic Analyzer (Applied Biosystems, Austin, TX).

DNA Sequencing

Sequencing was performed according to the manufacturer's instructions with Big Dye terminator version 3.1 and an ABI PRISM 3100 Genetic Analyzer (Applied Biosystems). Forward and reverse strands of all 38 *CC2D2A* exons were sequenced, as well as ~30 bp of flanking intronic sequence. Primers and conditions used are depicted in Table S1 available online.

Sequence Analysis

Alignments were performed with Clustal W2 and Boxshade 3.21. Homology calculations were performed with Vector NTI10 (Invitrogen Corporation, Carlsbad, CA). Phylogenetic trees were constructed with BLAST and TreeFam.

RT-PCR for Human Transcripts

Fetal eye and liver mRNA was isolated with the RNeasy Mini Kit (QIAgen, Valencia, CA) and all other RNAs were purchased: adult retina from Clontech (Mountain View, CA), adult brain, kidney, liver, heart, lung, and skeletal muscle from Ambion (Austin, TX), and fetal brain and kidney from Virogen (Watertown, MA). RT-PCR analysis of *CC2D2A*, *CC2D2B*, *RPGRIP1L*, and *HPRT* (control) was performed on total RNA from adult brain, retina, heart, kidney, liver, and skeletal muscle, as well as 12–16 week human fetal brain, eye, kidney, and liver. The primers are depicted in Table S1. Amplification was carried out in PCR buffer containing 2.5 mM $MgCl_2$ (32 cycles of denaturation for 30 s at 94°C, annealing for 30 s at 55°C [50°C for *RPGRIP1L*], and extension for 1 min at 72°C, with an initial denaturation step for 4 min at 94°C). The number of cycles was titrated so that the amount of product was not saturated in any tissue.

Immunocytochemistry

hTERT-RPE1 cells (kindly provided by Uwe Wolfrum) were cultured as described previously[19] and stained with anti-CEP290 (rabbit polyclonal, kindly provided by Erich Nigg) 1:100 or GT-335 (mouse monoclonal, kindly provided by Carsten Janke) 1:1000. hTERT-RPE1 cells were seeded on glass slides, grown overnight, and then transfected for 24 hr with eCFP-*CC2D2A* with Effectene (QIAgen), according to manufacturer's instructions. Primary cilium formation in hTERT-RPE1 cells was induced by serum starvation (0.2% serum) for another 24 hr. Prior to fixation, ciliated hTERT-RPE1 cells were washed briefly in PBS, fixed in ice-cold methanol for 10 min, and blocked with 2% BSA in PBS for 20 min. Slides were incubated with the primary antibodies for 1 hr at room temperature and subsequently washed with PBS. Subsequently, slides were incubated with secondary antibodies that were described previously. Washing with PBS was repeated. Cells were then embedded in Vectashield with DAPI (Vector Laboratories, Burlingame, CA) and analyzed with a Zeiss Axio Imager Z1 fluorescence microscope equipped with a 63× objective lens (Carl Zeiss, Sliedrecht, The Netherlands). Optical sections were generated through structured illumination by inserting an ApoTome slider into the illumination path, followed by processing with AxioVision (Carl Zeiss) and Photoshop CS2 software (Adobe Systems, San Jose, CA).

Yeast Two-Hybrid

Fragments of CC2D2A were tested for binding with proteins associated with ciliary disorders or cilia function (Table S2). The

N-terminal region until the C2 domain (1–998 aa), the C2 domain with the remaining C-terminal part (992–1561 aa), and the C2 domain alone (992–1177 aa) were cloned in pAD as well as pBD Gateway-adapted vectors. Yeast two-hybrid screening with ciliary proteins was performed in both directions. The BD Yeastmaker kit (Clontech) was used for transformation of yeast strains PJ69-4alpha and PJ69-4A with pBD and pAD vectors, respectively, according to the manufacturer's protocol. Yeast strains were mated and cotransformed yeast colonies were selected on plates lacking leucine (-L) and tryptophan (-W). Activation of the reporter genes was detected on selection plates lacking histidine (-LWH) and adenine (-LWHA). In addition, X-β-gal colorimetric filter lift assays (LacZ reporter gene) were performed to confirm the interaction as described.[3]

GST Pull-Down

We cloned the part of CEP290 (coiled-coil domain 4-6 encoded by amino acid residues 703–1030) that interacts with CC2D2A by yeast two-hybrid experiments with pDEST15, and we transformed this plasmid in BL21-DE3 cells. IPTG (Sigma-Aldrich, St. Louis, MO) was used to induce the expression of N-terminally GST-tagged CEP290 or GST alone. Purification of GST-CEP290$^{cc4\text{-}6}$ (~78 kDa) or GST alone (~26 kDa) was performed as described.[3] Bacterial lysates were added to 50 μl of glutathione Sepharose 4B coupled beads (Amersham Biosciences, Piscataway, NJ). Beads were washed twice with 1× STE (10 mM Tris-HCl [pH 8.0]; 1 mM EDTA; 150 mM NaCl) and incubated for 2 hr. Beads were again washed twice and incubated for 2 hr with lysates of COS-1 cells expressing a Flag-tagged fragment of CC2D2A (amino acids 1–998 encoding the N-terminal part until the C2 domain), followed by five washes with Triton-X buffer (50 mM Tris-HCl [pH 7.5]; 150 mM NaCl; 0.5% Triton X-100). Finally, we added Laemmli Sample Buffer (Bio-Rad Laboratories, Hercules, CA) to the beads and performed western blotting with mouse anti-Flag (1:1000, clone M2; Sigma-Aldrich), secondary IRDye800 goat anti-mouse antibody (1:20,000; Rockland) and the ODYSSEY system (Li-Cor, Lincoln, NE), as described.[3]

RT-PCR Methods for Zebrafish Transcripts

All zebrafish work was performed under an approved protocol at the Fred Hutchinson Cancer Research Center. At 48 hpf, 40 *snl*/*snl* zebrafish were identified by the sinusoidal tail phenotype. Likewise, 40 *snl*/+ and +/+ fish from the same cross were pooled. Whole zebrafish embryos were homogenized by mortar and pestle and passed through QIAshredder columns (QIAgen). Total RNA was isolated from the homogenate with the RNeasy Mini Kit (QIAgen). cDNA was reverse transcribed from total RNA with random primers and reagents supplied in the RETROscript Kit (Ambion). Primers for *sentinel* and the *odc1* (ornithine decarboxylase 1) housekeeping control gene are depicted in Table S1. Amplification was carried out for 34 cycles.

Genotyping for ZF

dCAP primers at the site of the sentinel mutation were designed to create an EcoRV restriction enzyme site in the PCR product from wild-type fish. Zebrafish genomic DNA was isolated with standard techniques. We used an annealing temperature of 64°C for 35 amplification cycles. Digested fragments were analyzed on 2% agarose gels.

Antibody Staining

Zebrafish embryos were fixed in Dent's fix (80% methanol/20% DMSO) at 4°C overnight. After gradual rehydration, they were washed several times in PBST (1× PBS with 0.5% Tween20) and blocked in PBS-DBT (1% DMSO/1% BSA/0.5% Tween20) with 10% normal sheep serum (NSS) (Sigma-Aldrich) at room temperature for 2 hr. Primary antibody incubation in PBS-DBT 10% NSS (1:2000 monoclonal anti-acetylated tubulin 6-11B-1 [Sigma-Aldrich]) was at 4°C overnight. Embryos were washed in PBST and blocked in PBS-DBT 10% NSS at RT for 1 hr and then incubated in 1:1000 goat anti-mouse Alexa Fluor 488 (Invitrogen) in PBS-DBT 10% NSS at 4°C overnight. After rinsing in PBS, the embryos were washed with methanol and equilibrated in clearing solution (1/3 benzoyl-alcohol and 2/3 benzoyl-benzoate) and examined with a Zeiss LSM510 confocal microscope.

Morpholino Injections

Antisense morpholino oligonucleotides blocking the function of CEP290[5] were obtained from GeneTools (Corvalis, OR). Morpholinos were diluted to a working concentration of 5 ng/nl in 0.2 M KCl, and 4 nl were pressure-injected into one- or two-cell stage zygotes.

Results

Homozygosity Mapping

To identify candidate loci for JSRD, we performed homozygosity mapping in consanguineous families with JSRD as described by Lander and Botstein.[25] The JSRD diagnosis was established by the presence of the MTS on brain MRI (Figures 1A–1E) and/or vermis hypoplasia on CT scan with supportive clinical findings: developmental delay/intellectual disability, ataxia, and/or abnormal eye movements. We genotyped affected and unaffected siblings in 28 consanguineous families with JSRD from multiple ethnic groups, with a cutoff of 80 consecutive homozygous SNPs to identify candidate regions of homozygosity in affected offspring of parents separated by six to nine meioses. Regions of homozygosity shared by affected and unaffected siblings were excluded. To further narrow these candidate regions, we also identified shared haplotypes of homozygous SNPs within and across families (Figures 1F–1H).

In Levanten Arab family UW50, we identified a shared haplotype of 252 consecutive homozygous SNPs spanning 7.6 Mb on chromosome 4p15 in two cousins, consistent with inheritance from a common ancestor (Figure 1F). These cousins shared no other regions of homozygosity greater than 50 consecutive homozygous SNPs, and the shared haplotype was heterozygous in available family members predicted to be obligate carriers. In Saudi Arabian families UW36 and UW48, the affected individuals shared a distinct haplotype of 64 consecutive homozygous SNPs at 4p15, providing additional evidence for a JSRD gene at this locus and narrowing the interval to 2.3 Mb (Figure 1G). The affected individuals did not share any other homozygous haplotypes greater than 38 consecutive SNPs. A fourth family (UW41) also had a large homozygous interval at chromosome 4p15 (Figure 1H). Segregation of the shared haplotype in each family was consistent with autosomal-recessive inheritance.

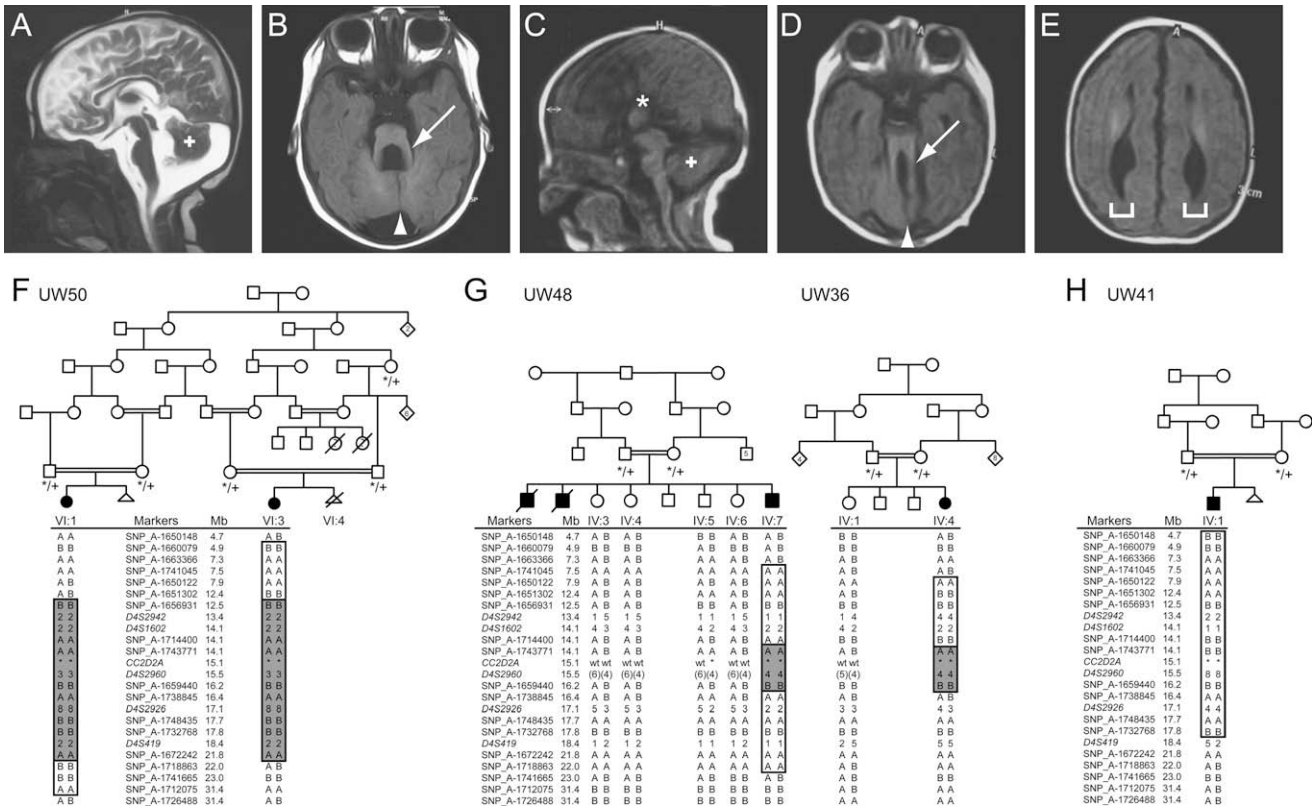

Figure 1. Homozygosity Mapping in Consanguineous Families with Joubert Syndrome

(A and B) Sagittal (A) and axial (B) MRI images of subject UW50 VI:3 revealing cerebellar vermis hypoplasia (arrowhead) and thick horizontally oriented superior cerebellar peduncles (arrow). (A) T2-weighted image; (B) T1-weighted image.

(C–E) Sagittal (C) and axial (D, E) MRI images of subject UW50 VI:1 revealing findings similar to subject UW50 VI:3. The midline tissue on the sagittal views (plus signs) is cerebellar hemisphere rather than vermis. Note the lack of corpus callosum (asterisk in [C]) and colpocephalic configuration of the lateral ventricles (brackets in [E]). T1-weighted images.

(F and G) Haplotypes at chromosome 4p15 locus in families UW50, UW48, UW36, and UW41. Mutations in *CC2D2A* are indicated by asterisks and known carriers are marked */+.

(F) Affected cousins in family UW50 share a haplotype of 242 consecutive homozygous SNPs (boxes) between SNP_A-1651302 and SNP_A-1718863 (9.6 Mb).

(G) Affected individuals in Saudi Arabian families UW36 and UW48 share a region of homozygosity (larger boxes) and a haplotype of 62 consecutive homozygous SNPs between SNP_A-1714400 and SNP_A-1738845 (2.3 Mb, smaller boxes). Unaffected siblings in UW48 are heterozygous in this region.

(H) The affected individual in family UW41 has a region of homozygosity between the 4p-terminus and D4S419. Note that only markers demarcating the regions of homozygosity and/or shared haplotypes are shown.

Mutation Detection

The 2.3 Mb shared haplotype in families UW36 and UW48 encompasses 14 genes (Figure 2A). We sequenced the coding regions and exon-intron boundaries of 13 of these genes in all four families, detecting two homozygous missense mutations (c.3364C → T p.P1122S; c.4582C → T p.R1528C) and one homozygous nonsense mutation (c.2848C → T p.R950X) in *CC2D2A* (Table 1 and Figure 3). As expected from the shared haplotype, we found that the two affected individuals in families UW36 and UW48 carry the same mutation (p.P1122S). P1122 is conserved across all species with related genes encoding this C2 domain, including all animals and protists, but not plants or fungi. R1528 is conserved in all vertebrates except pufferfish. Both missense mutations are predicted to be deleterious by SIFT and PolyPhen.[26,27] Sequence changes in the other 12 genes within the interval were either known SNPs or noncoding (not shown).

We then sequenced all *CC2D2A* exons in families that could not be excluded by segregation analysis by using four microsatellite markers at 4p15 (Figure 4). We identified compound heterozygous mutations in two families and a single frameshift mutation in a third nonconsanguineous family (Table 1 and Figure 3), yielding seven different *CC2D2A* mutations in 6 out of 70 JSRD families ascertained by the MTS ± other findings. A second cohort of 40 consanguineous JSRD families with renal disease was similarly evaluated, yielding one homozygous mutation (p.L1551P) in family F871, for a total prevalence of 7/110 (6%). The L1551P change is also predicted to be possibly damaging by Polyphen and tolerated by SIFT; however, this leucine is evolutionarily conserved as far as opossum, and proline

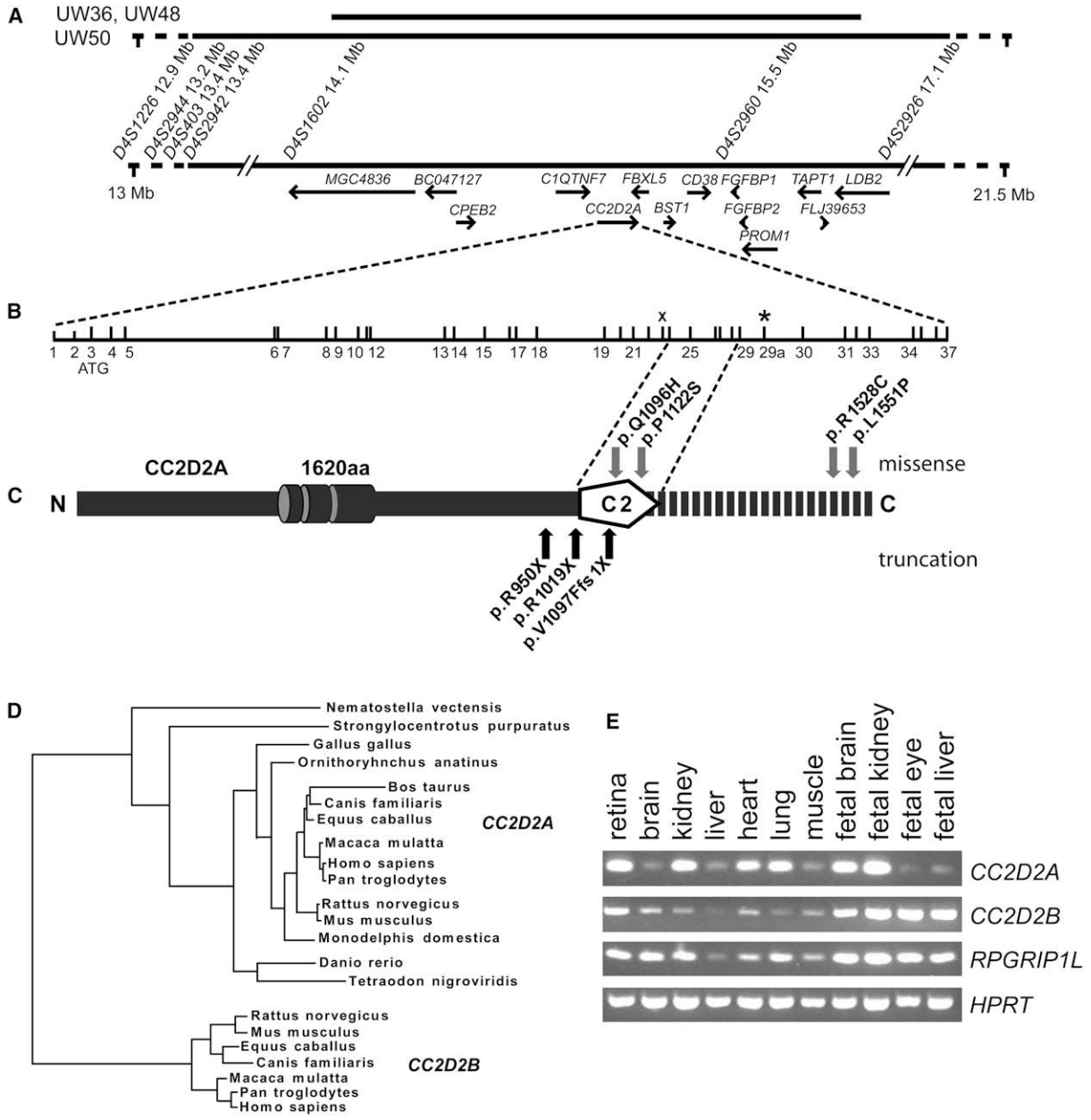

Figure 2. *CC2D2A* Locus, Gene, Predicted Protein, and Expression

(A) Map of chromosome 4p15 locus with the regions of homozygosity in affected members of families UW36, UW48, and UW50 indicated by horizontal lines. The genes within this interval are indicated by arrows.

(B) 37 predicted *CC2D2A* exons based on the UCSC genome browser. The position of the homozygous nonsense mutation in exon 23 (c.2848C → T p.R950X) is marked with an ×. Note that exon 29a (asterisk) is not included in the RefSeq gene sequence, but is found in at least two spliced ESTs and is highly conserved.

(C) The *CC2D2A* gene encodes a protein with three predicted coiled-coil domains (cylinders), as well as a single C2 domain (pentagon). Missense mutations (gray arrows) were present in the C2 domain and the highly conserved C-terminal region (broken bar), whereas protein-truncating mutations (black arrows) precede the C2 domain.

(D) Phylogenetic tree of the *CC2D2A* C2 domain reveals orthologs in diverse species and a *CC2D2B* paralog that is restricted to mammals.

(E) RT-PCR analysis of *CC2D2A*, *CC2D2B*, and *RPGRIP1L* expression in adult and fetal tissues. The *HPRT* (hypoxanthine phosphoribosyltransferase) gene was used as a template control.

is not present in any species. All mutations segregated as expected for autosomal-recessive inheritance, and the missense mutations were absent from >210 control chromosomes.

CC2D2A Mutations in Other Ciliopathies

We have shown recently that MKS genes contribute both primary loci and second site modifying alleles to the pathogenicity of BBS.[20] We therefore hypothesized that genes

Table 1. Mutations and Phenotypes in Subjects with *CC2D2A* Mutations

Affected Individual	Mutation(s)	Age (yr)	MRI/CT	Abnormal Eye Movements	Retinal Dystrophy	Coloboma	Renal Disease	Liver Fibrosis	Polydactyly	Encephalocele
UW36-IV:4	p.P1122S/p.P1122S	1	MTS	-	-[a]	-	-	-	-	-
UW46-II:1	p.V1097FfsX1/unknown	14	MTS	+	-	-	-	-	-	-
UW46-II:2	p.V1097FfsX1/unknown	17	MTS	+	-	-	-	-	-	-
UW47-II:1	p.R1019X/p.Q1096H	14	MTS	+	-	-	-	-	-	-
UW41-IV:1	p.R950X/p.R950X	4	MTS	+	+[b]	-	-	-	-	-
F871-II:1	p.L1551P/p.L1551P	8	VH	+	-	-	+	-	-	-
UW50-VI:1	p.R1528C/p.R1528C	4	MTS/ACC	-	-	-	-	-	-	+
UW50-VI:3	p.R1528C/p.R1528C	7	MTS	-	-	-	-	-	-	+[c]
UW48-IV:7	p.P1122S/p.P1122S	2.5	MTS	+	+	-	Abnormal RUS	Mild HSM	-	-
UW49-II:1	p.V1097FfsX1/p.R1528C	22	VH/ACC/HC	+	-	+	+[d]	+[e]	-	-

Affected individuals exhibit a spectrum of phenoptypes from isolated Joubert syndrome to COACH syndrome. MRI, magnetic resonance imaging; CT, computed tomography scan; MTS, molar tooth sign; VH, cerebellar vermis hypoplasia; ACC, agenesis of the corpus callosum; RUS, renal ultrasound; HSM, hepatosplenomegaly; HC, hydrocephalus. Minus sign indicates no overt signs of phenotype unless otherwise indicated.

[a] Normal electroretinogram (ERG).

[b] Flat ERG.

[c] In a fetal sibling.

[d] Mildly increased creatinine and upper normal renal echogenicity, no renal biopsy.

[e] Chronic inflammation and fibrosis of the portal triads, intact sinuses and central veins, required liver transplant at 10 years of age.

contributing to JSRD may also be involved in the manifestation of the BBS phenotype. To explore this possibility, we sequenced *CC2D2A* in 96 BBS patients preselected for having mutations in zero or one known causative ciliopathy locus. We detected one novel sequence variant, encoding a heterozygous K478E amino acid change in a European BBS family. Importantly, this variant is highly conserved as far as stickleback and predicted to be nontolerated by SIFT. Consistent with a potential modifying, but not causal, role in ciliary disease, we detected this variant in one of 192 ethnically matched control chromosomes; further investigations will be required to ascertain the potential effect of this allele on CC2D2A function. Overall, the paucity of novel variants identified in BBS patients suggests that *CC2D2A* is not a major contributor to BBS; however, screening of a larger or more ethnically diverse cohort will be necessary to test this possibility exhaustively.

In parallel, we also evaluated the potential role of *CC2D2A* in isolated nephronophthisis. By using homozygosity mapping, we excluded the 4p15 locus in 86 of 90 consanguineous families via a recessive model. In the four families that could not be excluded, we did not identify any *CC2D2A* mutations. These results indicate that *CC2D2A* mutations are not a major cause of isolated nephronophthisis.

Gene/Protein Structure

The 38 exon *CC2D2A* gene encodes a predicted 1620 amino acid product with coiled-coil and C2 domains (Figures 2B and 2C) described by Noor et al. and Tallila et al.[22,23] Tallila et al.[23] also reported an additional predicted exon between exons 29 and 30 that is not in the reference sequence (NM_001080522), whose presence we confirmed in multiple tissues via RT-PCR (not shown). The nonsense and frameshift mutations in JSRD patients precede the C2 domain and are likely to trigger nonsense-mediated decay, whereas the missense mutations occur in the C2 domain and C-terminal region, supporting a functional role for these parts of the protein (Figure 2C).

A human paralog (*CC2D2B*) is present on chromosome 10q23.33. Ensembl predicts a 322 amino acid CC2D2B product that corresponds to NP_001001732 and shares homology with the C-terminal region of CC2D2A; however, ESTs mapping to chromosome 10q23.33, comparison of the human genomic sequence to other mammals, and gene-prediction programs (reviewed in Brent[28]) reveal a 1341 amino acid predicted protein with 33% identity/46% similarity to CC2D2A (Figure S1). The C2 domains of CC2D2A and CC2D2B are 42% identical and 55% similar, whereas the C-terminal regions are 45% identical and 60% similar. *CC2D2A* orthologs are found in all vertebrates and in sea urchin, jellyfish, and insects, whereas *CC2D2B* orthologs are found only in mammals, implicating *CC2D2B* in processes restricted to this class (Figure 2D). Interestingly, the C-terminal region of both proteins is distantly related to the CEP76 protein, a component of the centrosome (Figure S2).[29]

Human Phenotype

We observed a spectrum of phenotypes in our cohort (Table 1). Subject UW49-II:1 has chorioretinal coloboma, renal, and liver disease (COACH phenotype). Liver biopsy displayed "chronic inflammation and fibrosis of the portal triads, intact sinuses, and central veins" and required living-related donor liver transplantation at 10 years of age. Her creatinine has been mildly elevated and her "renal echogenicity was in the upper limit of normal" on renal ultrasound, but she has not had a renal biopsy. Subject UW48-IV:7 may also have the COACH phenotype, but details of an abnormal renal ultrasound and mild hepatosplenomegaly are

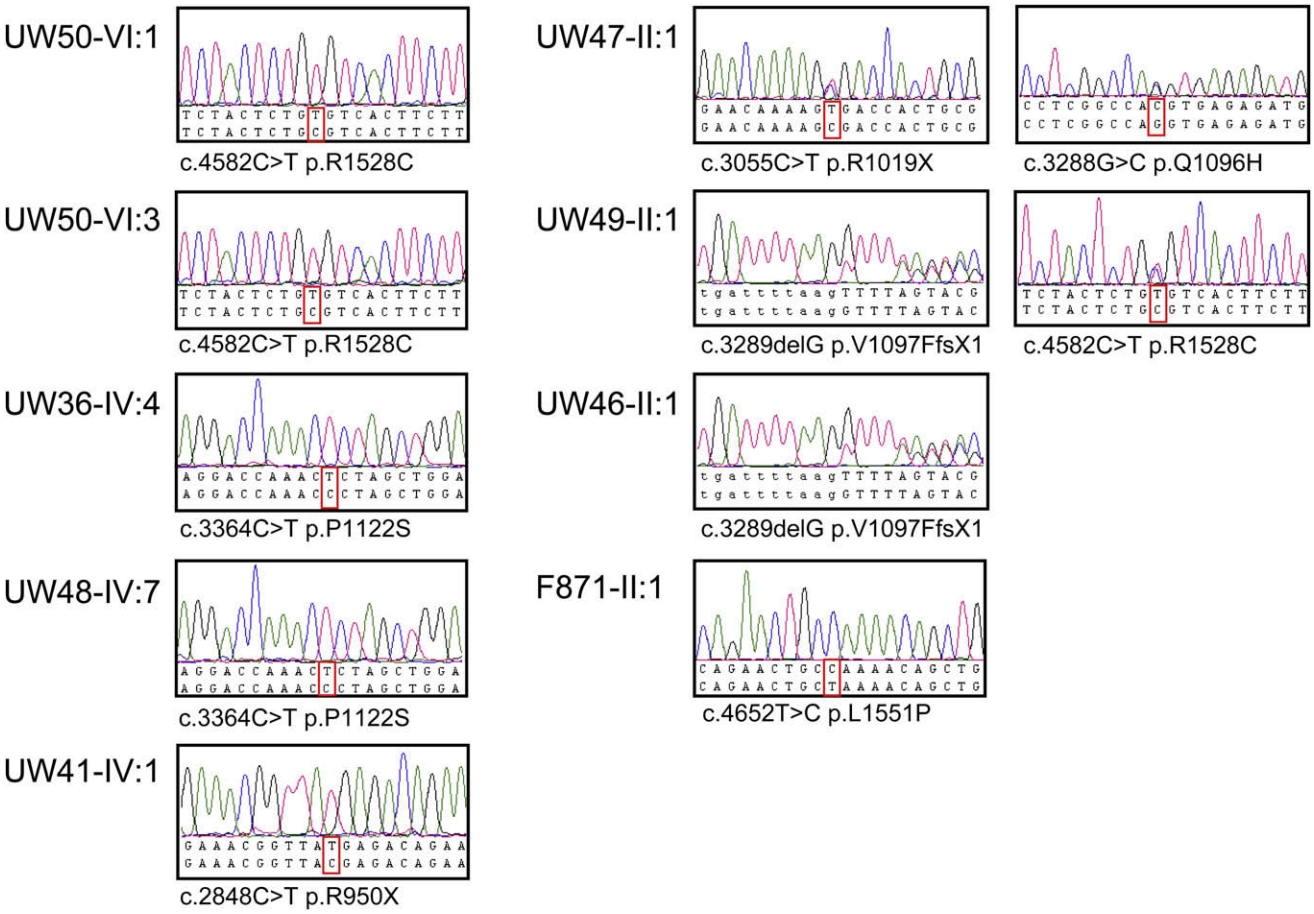

Figure 3. Sequence Tracings of *CC2D2A* Mutations
Numerical designations are based on NM_001080522.1 with the addition of exon 29a from genomic sequence (see Figure 2).

not available. Subjects UW48-IV:7 and UW41-IV:1 also have evidence of retinal dystrophy. Subjects UW50-VI:1 and UW50-VI:3 have encephaloceles similar to patients with MKS, whereas subjects UW50-VI:1 and UW49-II:1 have agenesis of the corpus callosum seen in a subset of individuals with JSRD. Affected individuals in UW36 and UW46 did not exhibit retinal, renal, or liver disease; however, UW36 was only 1 year old at last follow-up, and we found only a single CC2D2A mutation (p.V1097FfsX1) in UW46. No affected individuals had polydactyly. Although olfactory dysfunction has been observed in BBS,[30] it was not noted clinically in subjects with *CC2D2A* mutations, none of whom were formally tested for anosmia. After identifying *CC2D2A* mutations in subjects with JSRD, we reviewed the brain MRI images from two of the affected individuals with homozygous *CC2D2A* mutations described by Noor et al.,[22] and we identified the characteristic imaging features of Joubert syndrome in both subjects (one shown in Figures 4E and 4E′). No overt findings of liver or kidney disease were identified in this family.

Expression

CC2D2A transcript could not be detected via human multiple-tissue northern blots (not shown); however, we were able to detect transcript in all adult and fetal tissues tested via RT-PCR (Figure 2E). Interestingly, expression was substantially higher in fetal brain than in adult brain, which may indicate an increased requirement in this tissue during development. High levels of expression were also detected in retina and kidney, commonly affected in JSRD.

Colocalization of CC2D2A with CEP290 at the Basal Body

To investigate whether CC2D2A and CEP290 function in the same location, we transfected hTert-RPE1 cells with eCFP-tagged full-length *CC2D2A*. As described previously in COS-7 cells,[22] eCFP-CC2D2A is seen in the cytoplasm; however, after inducing cilia formation by serum starvation, eCFP-CC2D2A also localizes to the base of the cilia, as indicated by costaining with the anti-polyglutaminated tubulin antibody GT-335 (Figures 5A–5C). Costaining with CEP290 antibody[3] demonstrates that recombinant CC2D2A at the basal body colocalizes with endogenous CEP290 (Figures 5D–5F).

Physical Interaction between CC2D2A and CEP290

Based on the hypothesis that CC2D2A might function in the primary cilium/basal body protein network,[31] we

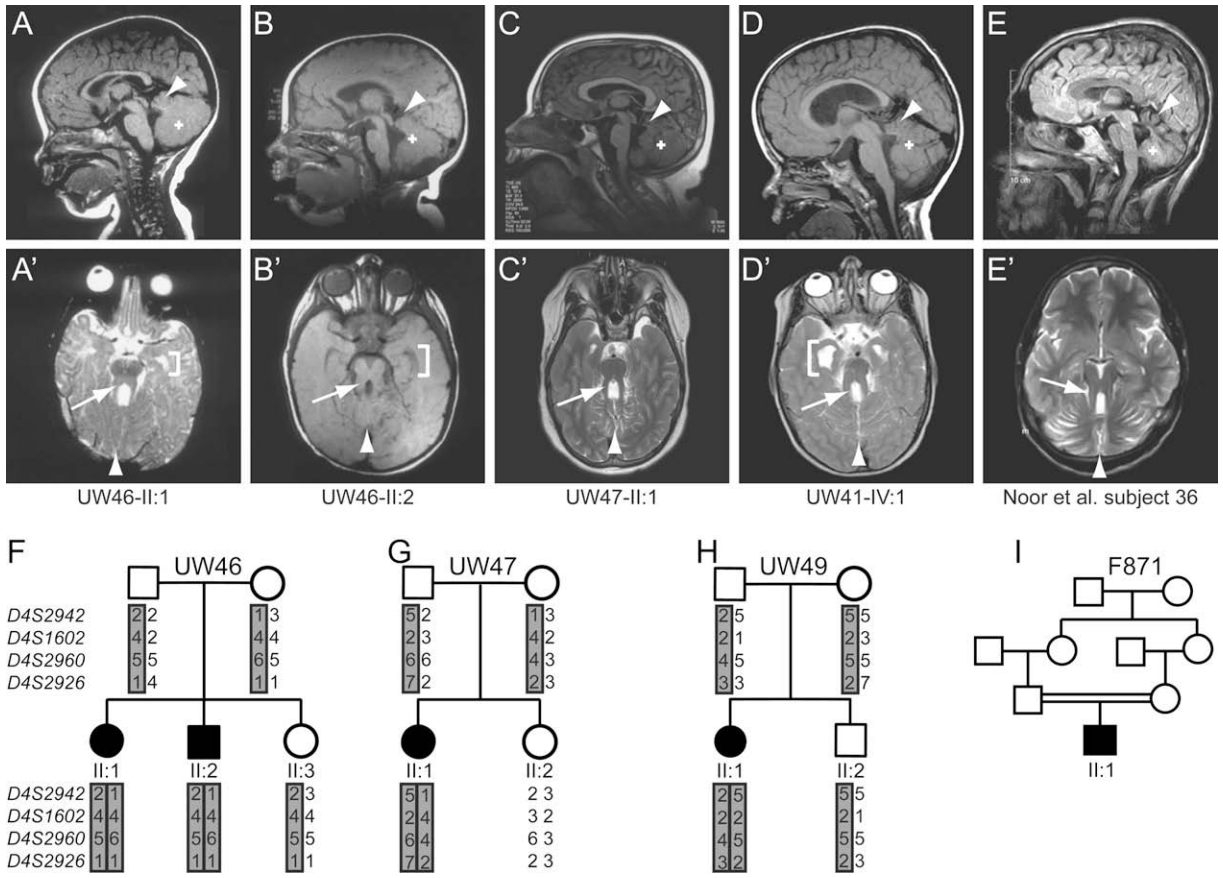

Figure 4. Segregation Analysis and MRI Images in Additional Families with *CC2D2A* Mutations

(A–E) Sagittal (A–E) and axial (A′–E′) MRI images of subjects UW46 II:1 (A, A′), UW46 II:2 (B, B′), UW47 II:1 (C, C′), UW41 II:1 (D, D′), and Noor et al. subject 36[22] (E, E′), revealing cerebellar vermis hypoplasia (arrowhead) and thick, horizontally oriented superior cerebellar peduncles (arrows). Mildly prominent temporal horns are bracketed in several axial images, consistent with mild ventriculomegaly. The cerebellar hemispheres in subject 36 appear atrophic (E′). (A–D, B′) T1-weighted images; (E) a T2/FLAIR-weighted image; (A′, C′–E′) T2-weighted images.

(F–H) Chromosome 4p15 could not be excluded by segregation of microsatellite markers in families UW46, UW47, and UW49.

(I) Pedigree for consanguineous family F871.

assessed 23 ciliopathy-associated proteins (including CEP290, RPGRIP1L, RPGRIP1, RPGR [MIM 312610], and BBS1-12 [MIM 209900]) for interaction with CC2D2A via a yeast two-hybrid mating assay (Table S2). These proteins were chosen on the basis of their involvement in a ciliopathy-associated protein network.[31] Of all combinations tested, only CEP290 was found to interact with CC2D2A (Figure 5G) and the interaction was confirmed by a GST pull-down assay (Figures 5H–5J). The interaction is specific for the N-terminal 998 amino acids of CC2D2A and an internal fragment of CEP290 (amino acids 703–1130) containing coiled-coil domains 4-6.

Modeling Loss of *cc2d2a* Function in Zebrafish

In a screen for mutations modifying aminoglycoside-induced mechanosensory hair cell damage, Owens et al. identified a nonsense mutation (*sentinel* [*snl*]) that lies N-terminal to the C2 domain in the sole zebrafish ortholog of *CC2D2A* (*cc2d2a*).[32] The Cc2d2a protein is more closely related to CC2D2A (60% identical, 74% similar) than CC2D2B (34% identical, 48% similar; Figure S1), with higher homology in the C2 domain and C-terminal region. We found that *cc2d2a* transcript is reduced substantially in *snl/snl* fish versus their wild-type and heterozygous siblings (Figure 6A), presumably because of nonsense-mediated decay. To further explore CC2D2A function and develop a zebrafish model for JSRD, we evaluated *snl/snl* fish for phenotypes reminiscent of JSRD and ciliary dysfunction including pronephric cysts, laterality defects, brain malformation, as well as defects in cilium number and morphology.[33] Although other obvious defects were not observed, 33% of the *snl/snl* fish (confirmed by genotyping) exhibited pronephric cysts by 6 days post-fertilization (dpf) compared to 0% of their wild-type and heterozygous siblings (Figures 6B and 6E). We used anti-acetylated tubulin antibody[34] to visualize motile cilia in the lumen of pronephric tubule and caudal region of the central canal. We were unable to discern any overt differences with respect to cilium number or morphology between *snl/snl* fish and their wild-type and heterozygous

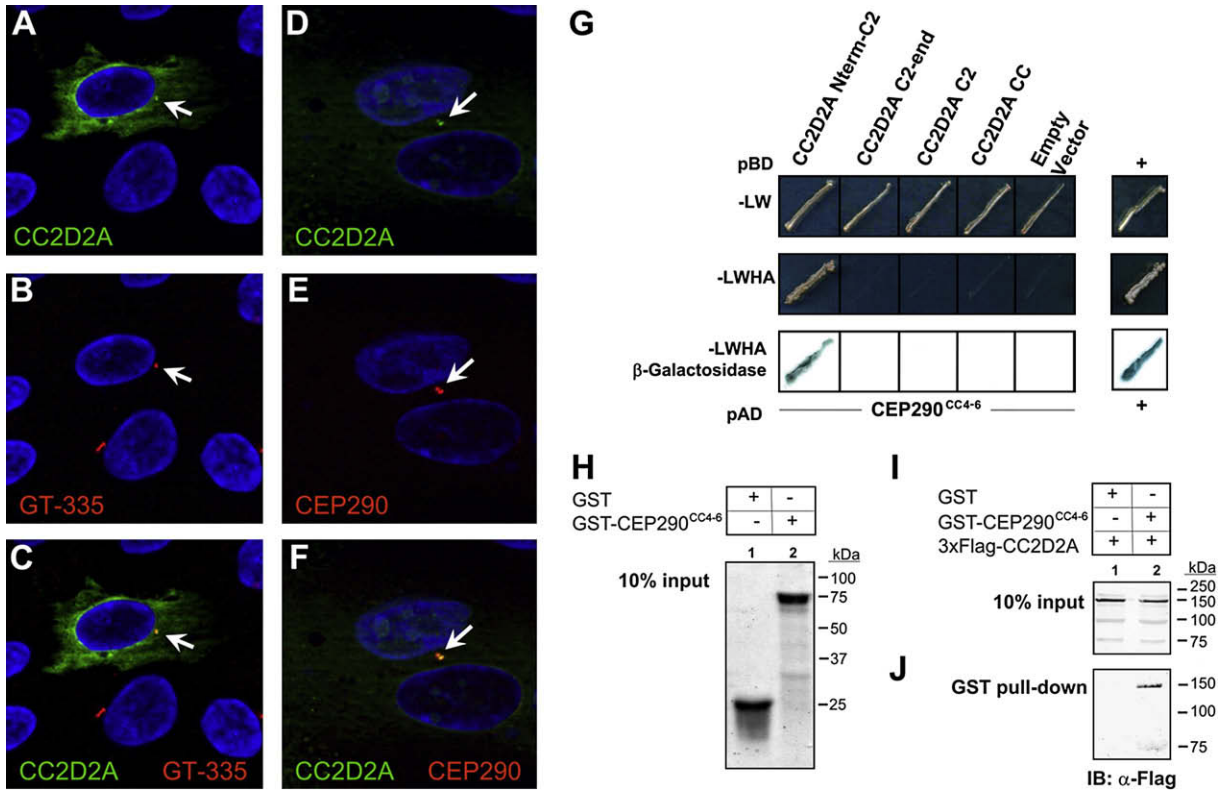

Figure 5. CC2D2A and CEP290 Colocalize at the Basal Body and Interact in Yeast Two-Hybrid Assay and GST Pull-Down

(A–C) Colocalization of eCFP-tagged CC2D2A (green) and ciliary marker GT-335, a mouse monoclonal antibody against polyglutaminated tubulin (red), in cultured retinal pigment epithelial cells (hTERT-RPE1). In addition to the specific localization to the basal body (arrows), eCFP-CC2D2A is also in the cytoplasm, possibly because of overexpression ([A and C], green).

(D–F) Colocalization of eCFP-tagged CC2D2A (green) and CEP290 (red) to the basal bodies (arrows) of cultured hTERT-RPE1 cells.

(G) CC2D2A interaction with CEP290 in a yeast two-hybrid assay. Bait plasmids expressing different fragments of CC2D2A as binding domain (BD)-fusion proteins were cotransformed in the PJ69-4 alpha yeast strain together with prey plasmids expressing CEP290 fragment CC4-6 (aa 703–1130) as activation domain (AD)-fusion proteins. Plates lacking the amino acids Leu and Trp (-LW, top) selected for cotransformants, whereas additional omission of His and Ade from the plates (-LWHA, middle) selected for activation of the cognate reporter genes. A blue color in the β-galactosidase filter lift assay (bottom) indicates activation of the LacZ reporter gene. All reporter genes were only activated by the interaction of the CC2D2A fragment Nterm-C2 (aa 1–998). The rightmost column (+) represents a positive control of the wild-type AD and BD domains.

(H–J) GST pull-down analysis of recombinant CC2D2A and CEP290 fragments.

(H) Expression of GST-alone (~26 kDa, lane 1) and GST-CEP290^{CC4-6} (amino acids 703–1030, which encode coiled-coil domains 4-6, ~78 kDa, lane 2). The Simply Blue-stained gel shows 10% of the input that was used in the GST pull-down experiment.

(I) Expression of 3xFlag-tagged CC2D2A$^{Nterm-C2}$ (amino acids 1–998, which encode the N-terminal domain until the C2 domain; lanes 1 and 2). The blot shows 10% of the input that was used in the GST pull-down.

(J) GST-CEP290^{CC4-6} specifically pulls down 3xFlag-CC2D2A$^{Nterm-C2}$ (band at 150 kDa, lane 2), whereas GST alone does not (lane 1).

siblings at 48 hpf, although subtle differences could not be excluded.

Functional Interaction with *CEP290*

To assess the functional significance of the CC2D2A-CEP290 physical interaction, we evaluated the effects of decreased *cep290* function in the *snl/snl* background. Sayer et al. found that knockdown of cep290 function in zebrafish via *cep290* morpholinos resulted in pronephric cyst formation,[5] so we titrated splice blocking (cep290splMO) and translation blocking (cep290atgMO) morpholinos to give a low prevalence of pronephric cysts in wild-type fish. We then injected offspring of a *snl*/+♂ × *snl*/+♀ cross and observed a striking exacerbation of the cyst phenotype in injected *snl/snl* fish compared to their injected siblings (*snl*/+ and +/+) and uninjected *snl/snl* fish (Figures 6B–6E). The cysts were larger, more prevalent, and evident 2 days earlier in the injected *snl/snl* fish, suggesting the cooperative action of CC2D2A and CEP290 in the pronephros. Cilia in injected *snl/snl* fish also appeared similar in morphology and number compared to wild-type.

Discussion

Coding mutations in *CC2D2A* account for 6/70 families (9%) in a cohort of JSRD families with consanguinity or

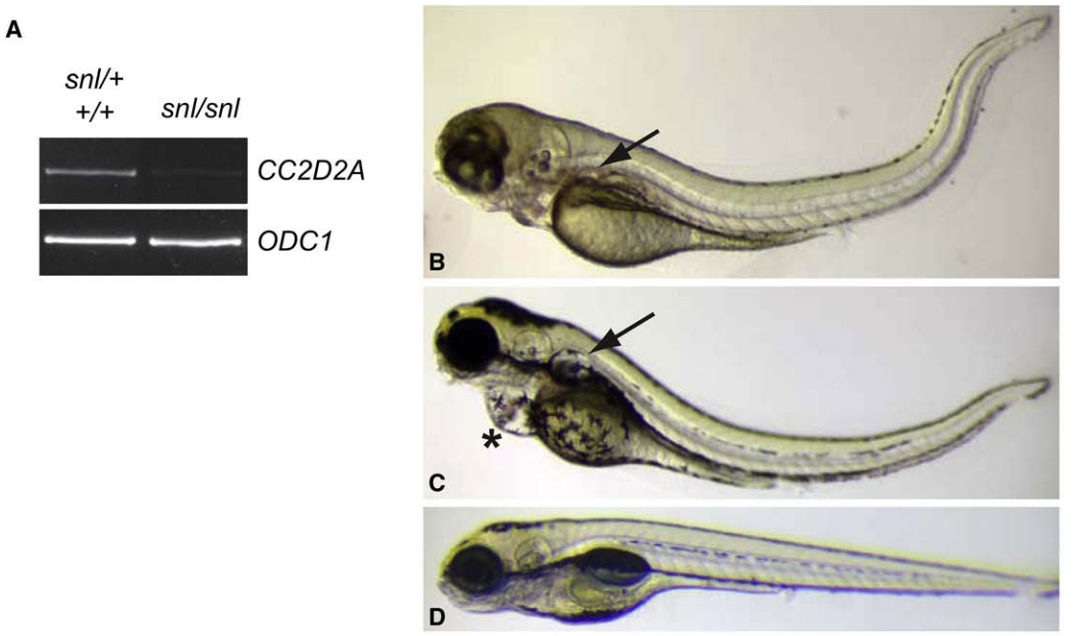

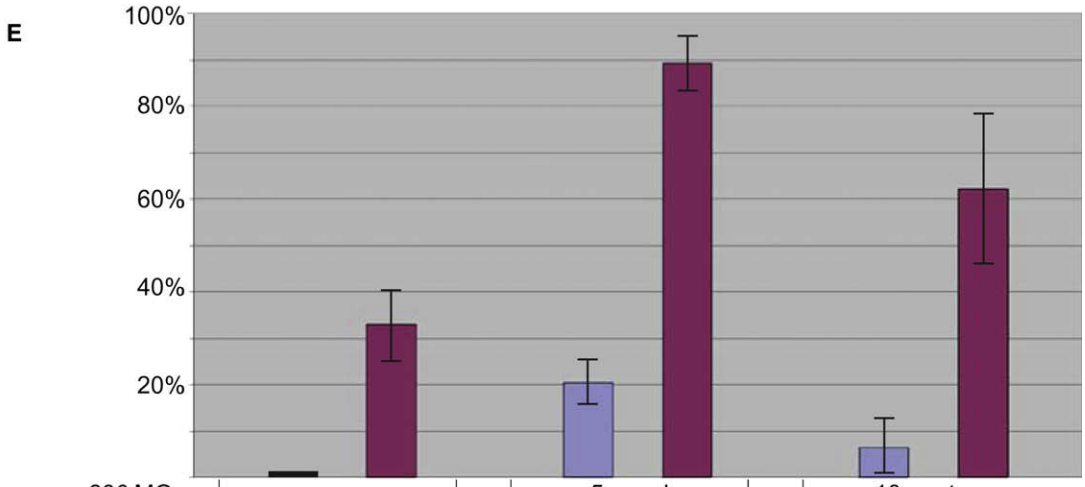

cep290 MO	none		5ng spl		10ng atg	
Genotype	*snl/+* and *+/+*	*snl/snl*	*snl/+* and *+/+*	*snl/snl*	*snl/+* and *+/+*	*snl/snl*
Fish with cysts	0	48	47	74	4	23
Total fish	490	146	231	83	61	37
% cysts	0	33	20	89	7	62

Figure 6. Zebrafish *sentinel* Phenotype and Synergistic Genetic Interaction with *cep290*

(A) *cc2d2a* expression is greatly reduced in *snl/snl* fish versus their *snl/+* and *+/+* siblings. The *odc1* gene was used as a template control.

(B and C) Tail and pronephros phenotype in *snl/snl* fish (B) and *snl/snl* fish injected with cep290splMO (C) at 4 dpf. *snl/snl* fish (B) have a sinusoidal-shaped tail and develop pronephric cysts (arrows) starting at 4 dpf, whereas *snl/snl* fish injected with cep290splMO (C) develop larger pronephric cysts starting at 2 dpf. Some of these fish also develop pericardial effusion (asterisk).

(D) AB wild-type fish for comparison.

(E) Frequency of pronephric cysts in *snl/snl* fish and their wild-type siblings (*snl/+* and *+/+*) with and without cep290splMO. Brackets indicate 95% confidence intervals ($p < 0.0001$ for comparison between *snl/snl* fish and their wild-type siblings [*snl/+* and *+/+*] injected with either CEP290 morpholino; chi-square test). dpf, days postfertilization; cep290splMO, *cep290* splice-blocking morpholino.

more than one offspring, making *CC2D2A* a major contributor to JSRD, similar to *AHI1* and *CEP290*.[5,35] We observed a broad spectrum of phenotypes in our subjects with *CC2D2A* mutations, including uncomplicated Joubert syndrome, the COACH subtype of JSRD,[2] and individuals with features overlapping with MKS (encephalocele and liver disease). Noor et al. reported a splice-site mutation segregating in a family now shown to have JSRD rather than autosomal-recessive mental retardation and retinitis pigmentosa.[22] In fetuses with MKS from a Finnish cohort,

Tallila et al. reported a single homozygous splice-site mutation that affects splicing and truncates CC2D2A earlier in the protein than any of the mutations in our series.[23] This offers a suggestion of genotype-phenotype correlation; however, the mutation predicted to be the most severe in our cohort (p.R950X prior to the C2 domain in family UW41) is associated with a relatively mild phenotype (no renal or liver disease), indicating that other factors, such as extragenic modifiers, are playing a role as they do in other ciliopathies.[36–38] In addition, subjects UW50-VI:1 and UW50-VI:3, despite having the same mutation, are discordant for agenesis of the corpus callosum. Subjects UW36-IV:4 and UW48-IV:7 also share the same mutation (P1122S) but are discordant for retinal dystrophy and potentially, for renal and liver disease. These observations provide support for the idea that JSRD and MKS are allelic disorders and that the liver fibrosis phenotype in COACH syndrome represents the milder end of the spectrum from the more severe ductal plate malformation seen in MKS.[39]

The pronephric cyst phenotype in *sentinel* fish is similar to that seen in other zebrafish with cilium dysfunction[33] and partially recapitulates the human JSRD phenotype. In contrast to the absence of primary cilia in cultured fibroblasts from fetuses with MKS reported by Tallila et al.,[23] we did not observe defects in the pronephric cilia of homozygous *snl* fish. It may be that the zebrafish mutation is less severe than the human mutation; however, the two mutations are both predicted to truncate the protein just after the predicted coiled-coil domains and before the C2 domain. Alternatively, *cc2d2a* function may be required for formation/maintenance of human fibroblast cilia but not zebrafish pronephros cilia. The connection between JSRD in humans and aminoglycoside resistance of mechanosensory hair cells in zebrafish is mysterious. Hearing loss is not a typical feature of JSRD and given the rarity of JSRD patients, demonstrating resistance to aminoglycoside-induced hearing loss in humans with JSRD is not feasable. As yet, an in vitro assay for aminoglycoside resistance in easily available human tissues has not been developed; however, this could be the subject of future work to connect the human and zebrafish phenotypes and explore the mechanisms underlying JSRD and aminoglycoside resistance. The relationship between ciliary dysfunction and aminoglycoside resistance is also not obvious. Although zebrafish hair cells possess a microtubule-based kinocilium at their apical surface, this structure does not appear to be disrupted and mechanotransduction appears normal in *sentinel* mutants.[32] The first detectable defect in zebrafish hair cells exposed to neomycin is a loss of mitochondrial potential and mitochondrial swelling.[40] It remains to be determined whether *CC2D2A* mutations block the toxic effect of aminoglycosides on the mitochondria, decrease the sensitivity of hair cells to mitochondrial dysfunction/energy starvation, or prevent hair cell damage by other mechanisms.

Our data suggest a functional role for CC2D2A at the basal body, closely associated with CEP290. We show that recombinant eCFP-CC2D2A colocalizes with CEP290 to the basal body in cultured ciliated cells, and the two proteins may directly interact, because the recombinant proteins are able to physically bind. Ideally, these experiments will need to be confirmed on endogenous proteins via antibodies to CC2D2A, especially because GST pull-down assays showed affinity between recombinant CC2D2A and other higher-molecular-weight proteins (results not shown). A variety of evidence provides additional support for the role of CC2D2A at the basal body. *CC2D2A* encodes a coiled-coil and C2 calcium/lipid binding domain protein included in the cilium/basal body proteome.[41] Despite a lack of direct sequence homology, CC2D2A has a strikingly similar overall structure to RPGRIP1L and RPGRIP1, two basal body proteins defective in JSRD/MKS and LCA.[3,4,21] The loss-of-function phenotype for *CC2D2A* overlaps with other disorders of ciliary function in humans and zebrafish. Tallila et al. found that cilia were absent from fibroblasts cultured from fetuses with an early truncating mutation in *CC2D2A*.[23] The *C. elegans* (K07G5.3) and *D. melanogaster* (CG18631) *CC2D2A* orthologs each have an xbox sequence in their promoter region, predicted to bind DAF-19, a transcription factor involved in regulation of a broad spectrum of ciliary genes.[42–44] The CC2D2A C-terminal region is also similar to CEP76, another widely conserved C2 domain protein that is present in the centrosome and required in the cilium.[19,29] Furthermore, CC2D2A was identified in a screen for proteins that interact with calmodulin,[45] raising the possibility that CC2D2A participates in calcium-dependent signaling pathways and the network of proteins required for retinal photoreceptor development/function, including CEP290, RPGR, RPGRIP1, RPGRIP1L, NPHP4 (MIM 607215), and NPHP5 (MIM 609237).[46]

In conclusion, we demonstrate that *CC2D2A* is responsible for a substantive proportion of JSRD including cases with the distinctive COACH subtype that likely represents a transitional phenotype between JSRD and MKS. Furthermore, *CC2D2A* functions in close association with *CEP290* and provides a model for studying the impact of an extragenic modifier (i.e., decreased *CEP290* function) on the phenotypes resulting from mutations in a causal gene (*CC2D2A*).

Supplemental Data

Supplemental Data include two figures and two tables and can be found with this article online at http://www.ajhg.org/.

Acknowledgments

We thank all the participating families with Joubert syndrome and M. Landsverk, R. Howard, J. Adkins, and members of the Moens laboratory for expert technical assistance and helpful discussions. This work was supported by the US National Institutes of Health (grants K23NS45832 to M.A.P., K24HD46712 to I.A.G., NCRR 5KL2RR025015 to D.D., and P30ES07033 to F.M.F.), the University of Washington Center on Human Development and Disability

(P30HD02274 to D.D., M.A.P., and I.A.G.), Howard Hughes Medical Institute (to C.B.M.), the University of Washington Center on Ecogenetics and Environmental Health and the March of Dimes Endowment for Healthier Babies at Children's Hospital in Seattle (to D.D., M.A.P., and I.A.G.), as well as grants from the Dutch Kidney Foundation (C04.2112 to N.V.A.M.K. and R.R.), EVI-GENORET (LSHG-CT-2005 512036 to R.R.), and the Netherlands Organisation for Scientific Research (NWO Vidi-91786396 to R.R. and NWO Toptalent-021.001.014 to K.L.M.C.).

Received: July 4, 2008
Revised: October 1, 2008
Accepted: October 2, 2008
Published online: October 23, 2008

Web Resources

The URLs for data presented herein are as follows:

BLAST, http://www.ncbi.nlm.nih.gov/blast/Blast.cgi
Boxshade 3.21, http://www.ch.embnet.org/software/BOX_form.html
Clustal W2, http://www.ebi.ac.uk/Tools/clustalw2/index.html
Online Mendelian Inheritance in Man (OMIM), http://www.ncbi.nlm.nih.gov/Omim/
TreeFam, http://www.treefam.org/

References

1. Parisi, M.A., Doherty, D., Chance, P.F., and Glass, I.A. (2007). Joubert syndrome (and related disorders) (OMIM 213300). Eur. J. Hum. Genet. *15*, 511–521.
2. Verloes, A., and Lambotte, C. (1989). Further delineation of a syndrome of cerebellar vermis hypo/aplasia, oligophrenia, congenital ataxia, coloboma, and hepatic fibrosis. Am. J. Med. Genet. *32*, 227–232.
3. Arts, H.H., Doherty, D., van Beersum, S.E., Parisi, M.A., Letteboer, S.J., Gorden, N.T., Peters, T.A., Marker, T., Voesenek, K., Kartono, A., et al. (2007). Mutations in the gene encoding the basal body protein RPGRIP1L, a nephrocystin-4 interactor, cause Joubert syndrome. Nat. Genet. *39*, 882–888.
4. Delous, M., Baala, L., Salomon, R., Laclef, C., Vierkotten, J., Tory, K., Golzio, C., Lacoste, T., Besse, L., Ozilou, C., et al. (2007). The ciliary gene RPGRIP1L is mutated in cerebello-oculo-renal syndrome (Joubert syndrome type B) and Meckel syndrome. Nat. Genet. *39*, 875–881.
5. Sayer, J.A., Otto, E.A., O'Toole, J.F., Nurnberg, G., Kennedy, M.A., Becker, C., Hennies, H.C., Helou, J., Attanasio, M., Fausett, B.V., et al. (2006). The centrosomal protein nephrocystin-6 is mutated in Joubert syndrome and activates transcription factor ATF4. Nat. Genet. *38*, 674–681.
6. Baala, L., Romano, S., Khaddour, R., Saunier, S., Smith, U.M., Audollent, S., Ozilou, C., Faivre, L., Laurent, N., Foliguet, B., et al. (2007). The Meckel-Gruber syndrome gene, MKS3, is mutated in Joubert syndrome. Am. J. Hum. Genet. *80*, 186–194.
7. Dawe, H.R., Smith, U.M., Cullinane, A.R., Gerrelli, D., Cox, P., Badano, J.L., Blair-Reid, S., Sriram, N., Katsanis, N., Attie-Bitach, T., et al. (2007). The Meckel-Gruber Syndrome proteins MKS1 and meckelin interact and are required for primary cilium formation. Hum. Mol. Genet. *16*, 173–186.
8. Otto, E.A., Schermer, B., Obara, T., O'Toole, J.F., Hiller, K.S., Mueller, A.M., Ruf, R.G., Hoefele, J., Beekmann, F., Landau, D., et al. (2003). Mutations in INVS encoding inversin cause nephronophthisis type 2, linking renal cystic disease to the function of primary cilia and left-right axis determination. Nat. Genet. *34*, 413–420.
9. Parisi, M.A., Bennett, C.L., Eckert, M.L., Dobyns, W.B., Gleeson, J.G., Shaw, D.W., McDonald, R., Eddy, A., Chance, P.F., and Glass, I.A. (2004). The NPHP1 gene deletion associated with juvenile nephronophthisis is present in a subset of individuals with Joubert syndrome. Am. J. Hum. Genet. *75*, 82–91.
10. Eley, L., Gabrielides, C., Adams, M., Johnson, C.A., Hildebrandt, F., and Sayer, J.A. (2008). Jouberin localizes to collecting ducts and interacts with nephrocystin-1. Kidney Int., in press.
11. Graber, D., Antignac, C., Deschenes, G., Coulin, A., Hermouet, Y., Pedespan, J.M., Fontan, D., and Ponsot, G. (2001). Cerebellar vermis hypoplasia with extracerebral involvement (retina, kidney, liver): difficult to classify syndromes. Arch. Pediatr. *8*, 186–190.
12. Takano, K., Nakamoto, T., Okajima, M., Sudo, A., Uetake, K., and Saitoh, S. (2003). Cerebellar and brainstem involvement in familial juvenile nephronophthisis type I. Pediatr. Neurol. *28*, 142–144.
13. Cantagrel, V., Silhavy, J.L., Bielas, S.L., Swistun, D., Marsh, S.E., Bertrand, J.Y., Audollent, S., Attie-Bitach, T., Holden, K.R., Dobyns, W.B., et al. (2008). Mutations in the cilia gene ARL13B lead to the classical form of Joubert syndrome. Am. J. Hum. Genet. *83*, 170–179.
14. Badano, J.L., Mitsuma, N., Beales, P.L., and Katsanis, N. (2006). The ciliopathies: An emerging class of human genetic disorders. Annu. Rev. Genomics Hum. Genet. *7*, 125–148.
15. Adams, M., Smith, U.M., Logan, C.V., and Johnson, C.A. (2008). Recent advances in the molecular pathology, cell biology and genetics of ciliopathies. J. Med. Genet. *45*, 257–267.
16. Valente, E.M., Silhavy, J.L., Brancati, F., Barrano, G., Krishnaswami, S.R., Castori, M., Lancaster, M.A., Boltshauser, E., Boccone, L., Al-Gazali, L., et al. (2006). Mutations in CEP290, which encodes a centrosomal protein, cause pleiotropic forms of Joubert syndrome. Nat. Genet. *38*, 623–625.
17. den Hollander, A.I., Koenekoop, R.K., Yzer, S., Lopez, I., Arends, M.L., Voesenek, K.E., Zonneveld, M.N., Strom, T.M., Meitinger, T., Brunner, H.G., et al. (2006). Mutations in the CEP290 (NPHP6) gene are a frequent cause of Leber congenital amaurosis. Am. J. Hum. Genet. *79*, 556–561.
18. Baala, L., Audollent, S., Martinovic, J., Ozilou, C., Babron, M.C., Sivanandamoorthy, S., Saunier, S., Salomon, R., Gonzales, M., Rattenberry, E., et al. (2007). Pleiotropic effects of CEP290 (NPHP6) mutations extend to Meckel syndrome. Am. J. Hum. Genet. *81*, 170–179.
19. Graser, S., Stierhof, Y.D., Lavoie, S.B., Gassner, O.S., Lamla, S., Le Clech, M., and Nigg, E.A. (2007). Cep164, a novel centriole appendage protein required for primary cilium formation. J. Cell Biol. *179*, 321–330.
20. Leitch, C.C., Zaghloul, N.A., Davis, E.E., Stoetzel, C., Diaz-Font, A., Rix, S., Al-Fadhel, M., Lewis, R.A., Eyaid, W., Banin, E., et al. (2008). Hypomorphic mutations in syndromic encephalocele genes are associated with Bardet-Biedl syndrome. Nat. Genet. *40*, 443–448.
21. Dryja, T.P., Adams, S.M., Grimsby, J.L., McGee, T.L., Hong, D.H., Li, T., Andreasson, S., and Berson, E.L. (2001). Null RPGRIP1 alleles in patients with Leber congenital amaurosis. Am. J. Hum. Genet. *68*, 1295–1298.

22. Noor, A., Windpassinger, C., Patel, M., Stachowiak, B., Mikhailov, A., Azam, M., Irfan, M., Siddiqui, Z.K., Naeem, F., Paterson, A.D., et al. (2008). CC2D2A, encoding a coiled-coil and C2 domain protein, causes autosomal-recessive mental retardation with retinitis pigmentosa. Am. J. Hum. Genet. *82*, 1011–1018.
23. Tallila, J., Jakkula, E., Peltonen, L., Salonen, R., and Kestila, M. (2008). Identification of CC2D2A as a Meckel syndrome gene adds an important piece to the ciliopathy puzzle. Am. J. Hum. Genet. *82*, 1361–1367.
24. Beales, P.L., Elcioglu, N., Woolf, A.S., Parker, D., and Flinter, F.A. (1999). New criteria for improved diagnosis of Bardet-Biedl syndrome: Results of a population survey. J. Med. Genet. *36*, 437–446.
25. Lander, E.S., and Botstein, D. (1987). Homozygosity mapping: a way to map human recessive traits with the DNA of inbred children. Science *236*, 1567–1570.
26. Ramensky, V., Bork, P., and Sunyaev, S. (2002). Human non-synonymous SNPs: server and survey. Nucleic Acids Res. *30*, 3894–3900.
27. Ng, P.C., and Henikoff, S. (2003). SIFT: Predicting amino acid changes that affect protein function. Nucleic Acids Res. *31*, 3812–3814.
28. Brent, M.R. (2008). Steady progress and recent breakthroughs in the accuracy of automated genome annotation. Natl. Rev. *9*, 62–73.
29. Andersen, J.S., Wilkinson, C.J., Mayor, T., Mortensen, P., Nigg, E.A., and Mann, M. (2003). Proteomic characterization of the human centrosome by protein correlation profiling. Nature *426*, 570–574.
30. Kulaga, H.M., Leitch, C.C., Eichers, E.R., Badano, J.L., Lesemann, A., Hoskins, B.E., Lupski, J.R., Beales, P.L., Reed, R.R., and Katsanis, N. (2004). Loss of BBS proteins causes anosmia in humans and defects in olfactory cilia structure and function in the mouse. Nat. Genet. *36*, 994–998.
31. Roepman, R., and Wolfrum, U. (2007). Protein networks and complexes in photoreceptor cilia. Subcell. Biochem. *43*, 209–235.
32. Owens, K.N., Santos, F., Roberts, B., Linbo, T., Coffin, A.B., Knisely, A.J., Simon, J.A., Rubel, E.W., and Raible, D.W. (2008). Identification of genetic and chemical modulators of zebrafish mechanosensory hair cell death. PLoS Genet. *4*, e1000020.
33. Kramer-Zucker, A.G., Olale, F., Haycraft, C.J., Yoder, B.K., Schier, A.F., and Drummond, I.A. (2005). Cilia-driven fluid flow in the zebrafish pronephros, brain and Kupffer's vesicle is required for normal organogenesis. Development *132*, 1907–1921.
34. Piperno, G., and Fuller, M.T. (1985). Monoclonal antibodies specific for an acetylated form of alpha-tubulin recognize the antigen in cilia and flagella from a variety of organisms. J. Cell Biol. *101*, 2085–2094.
35. Parisi, M.A., Doherty, D., Eckert, M.L., Shaw, D.W., Ozyurek, H., Aysun, S., Giray, O., Al Swaid, A., Al Shahwan, S., Dohayan, N., et al. (2006). AHI1 mutations cause both retinal dystrophy and renal cystic disease in Joubert syndrome. J. Med. Genet. *43*, 334–339.
36. Badano, J.L., Leitch, C.C., Ansley, S.J., May-Simera, H., Lawson, S., Lewis, R.A., Beales, P.L., Dietz, H.C., Fisher, S., and Katsanis, N. (2006). Dissection of epistasis in oligogenic Bardet-Biedl syndrome. Nature *439*, 326–330.
37. Hoefele, J., Wolf, M.T., O'Toole, J.F., Otto, E.A., Schultheiss, U., Deschenes, G., Attanasio, M., Utsch, B., Antignac, C., and Hildebrandt, F. (2007). Evidence of oligogenic inheritance in nephronophthisis. J. Am. Soc. Nephrol. *18*, 2789–2795.
38. Katsanis, N., Ansley, S.J., Badano, J.L., Eichers, E.R., Lewis, R.A., Hoskins, B.E., Scambler, P.J., Davidson, W.S., Beales, P.L., and Lupski, J.R. (2001). Triallelic inheritance in Bardet-Biedl syndrome, a Mendelian recessive disorder. Science *293*, 2256–2259.
39. Johnson, C.A., Gissen, P., and Sergi, C. (2003). Molecular pathology and genetics of congenital hepatorenal fibrocystic syndromes. J. Med. Genet. *40*, 311–319.
40. Owens, K.N., Cunningham, D.E., MacDonald, G., Rubel, E.W., Raible, D.W., and Pujol, R. (2007). Ultrastructural analysis of aminoglycoside-induced hair cell death in the zebrafish lateral line reveals an early mitochondrial response. J. Comp. Neurol. *502*, 522–543.
41. Gherman, A., Davis, E.E., and Katsanis, N. (2006). The ciliary proteome database: An integrated community resource for the genetic and functional dissection of cilia. Nat. Genet. *38*, 961–962.
42. Blacque, O.E., Perens, E.A., Boroevich, K.A., Inglis, P.N., Li, C., Warner, A., Khattra, J., Holt, R.A., Ou, G., Mah, A.K., et al. (2005). Functional genomics of the cilium, a sensory organelle. Curr. Biol. *15*, 935–941.
43. Efimenko, E., Bubb, K., Mak, H.Y., Holzman, T., Leroux, M.R., Ruvkun, G., Thomas, J.H., and Swoboda, P. (2005). Analysis of xbx genes in *C. elegans*. Development *132*, 1923–1934.
44. Avidor-Reiss, T., Maer, A.M., Koundakjian, E., Polyanovsky, A., Keil, T., Subramaniam, S., and Zuker, C.S. (2004). Decoding cilia function: Defining specialized genes required for compartmentalized cilia biogenesis. Cell *117*, 527–539.
45. Shen, X., Valencia, C.A., Szostak, J.W., Dong, B., and Liu, R. (2005). Scanning the human proteome for calmodulin-binding proteins. Proc. Natl. Acad. Sci. USA *102*, 5969–5974.
46. Otto, E.A., Loeys, B., Khanna, H., Hellemans, J., Sudbrak, R., Fan, S., Muerb, U., O'Toole, J.F., Helou, J., Attanasio, M., et al. (2005). Nephrocystin-5, a ciliary IQ domain protein, is mutated in Senior-Loken syndrome and interacts with RPGR and calmodulin. Nat. Genet. *37*, 282–288.